Polymer 41 (2000) 5541–5545

polymer

Polymer Communication

Micro-thermomechanical properties of heterogeneous polymer films

V.V. Tsukruk*, Z. Huang

Materials Science & Engineering Department, Iowa State University Ames, IA 50011, USA

Received 12 April 1999; accepted 19 December 1999

Abstract

We studied the surface distribution of the adhesive forces and elastic moduli for heterogeneous polymer films. Micromechanical properties of polysterene/polybutadyene (PS/PB) thin films were probed by scanning probe microscopy in a range of temperatures, from room temperature to above the glass transition of the PS matrix. We demonstrated that for heterogeneous composite films fabricated from polymer blends, the micromapping of surface properties can be obtained concurrently for glassy and rubber phases as well as across the interface with a lateral resolution better than 100 nm. Histograms of the surface distribution display two very distinctive maxima, which allows concurrent measurements of micromechanical properties of glassy and rubber phases. Depth profile measurements demonstrate the gradual increase of the rubber phase thickness with an increasing distance from the PS/PB interface. Glass transition temperature of the glassy matrix and the flow temperature of the rubber phase can be detected by this technique, and both temperatures are close to the known bulk values. © 2000 Elsevier Science Ltd. All rights reserved.

Keywords: Micromechanics; Scanning probe microscopy; Polymer blends

Knowledge of the surface/interfacial distribution of physical properties with a nanoscale resolution is critical for the design of nanocomposite polymeric materials and coatings. Mapping of micromechanical properties of polymer interfaces is a challenging problem and could not even be addressed before the invention of atomic force microscopy/scanning probe microscopy (AFM/SPM) in 1986 [1]. First attempts of extracting the nanomechanical properties from local indentation experiments were conducted according to the classical Sneddon's indentation approach [2,3]. Further developments lead to micromapping of surface mechanical properties with the so-called force modulation mode in various variants [4–7]. However, this mode probes micromechanical properties at unnaturally high frequencies (hundreds of kHz) as compared to the usual macroscopic measurements (Hz) [8]. This leads to significant shifts in the thermal transformations/moduli (tens of degrees/hundred percents of modulus) and makes the direct comparison of SPM and ordinary mechanical data very difficult.

Several studies were focused on the development of dc force–displacement probing of micromechanical properties [9–11]. This approach allows testing the micromechanical properties within the important frequency domain of 0.1–100 Hz. In our previous publications, we reported on the adoption of the known models of contact elastic deformation to the SPM technique [12–15]. We tested Hertzian's, Sneddon's, and Johnson–Kendall–Roberts's theories for a number of polymeric materials from rubber to polystyrene and received reliable and consistent results. In the present communication, we report on the microprobing/micromapping of *polymer composite materials* that provide a new insight on the fine details of micromechanics of polymer surfaces and interfaces.

Samples for investigation were prepared by spin-coating of polystyrene ($M_w = 250,000$, Janssen Chemical Co.)/polybutadiene ($M_w = 420,000$, Aldrich) (PS/PB) glass–rubber blends on a silicon wafer with PS as a matrix and PB as a dispersed phase. Films thickness was kept within 2–3 μm. Films were probed with a Dimension IIIA microscope (Digital Instruments) in a Force Volume mode with a probing frequency of 2 Hz and a lateral resolution of 32 × 32 or 64 × 64 pixels. The SPM tips were silicon tips with a spring constant determined by a combination of resonant frequency and spring-against-spring techniques [16–18]. Tip radius was measured by scanning gold nanoparticles [19]. Adhesive forces were calculated from pull-off points and elastic moduli were estimated by using the Hertzian model [12,13]. Details of data processing are described elsewhere [18,20].

As observed, PS/PB films are highly heterogeneous with well-developed phase separation of the rubber phase and

---

* Corresponding author. Tel.: +1-515-294-6904; fax: +1-515-294-5444.
E-mail address: vladimir@iastate.edu (V.V. Tsukruk).

PII: S0032-3861(00)00004-5

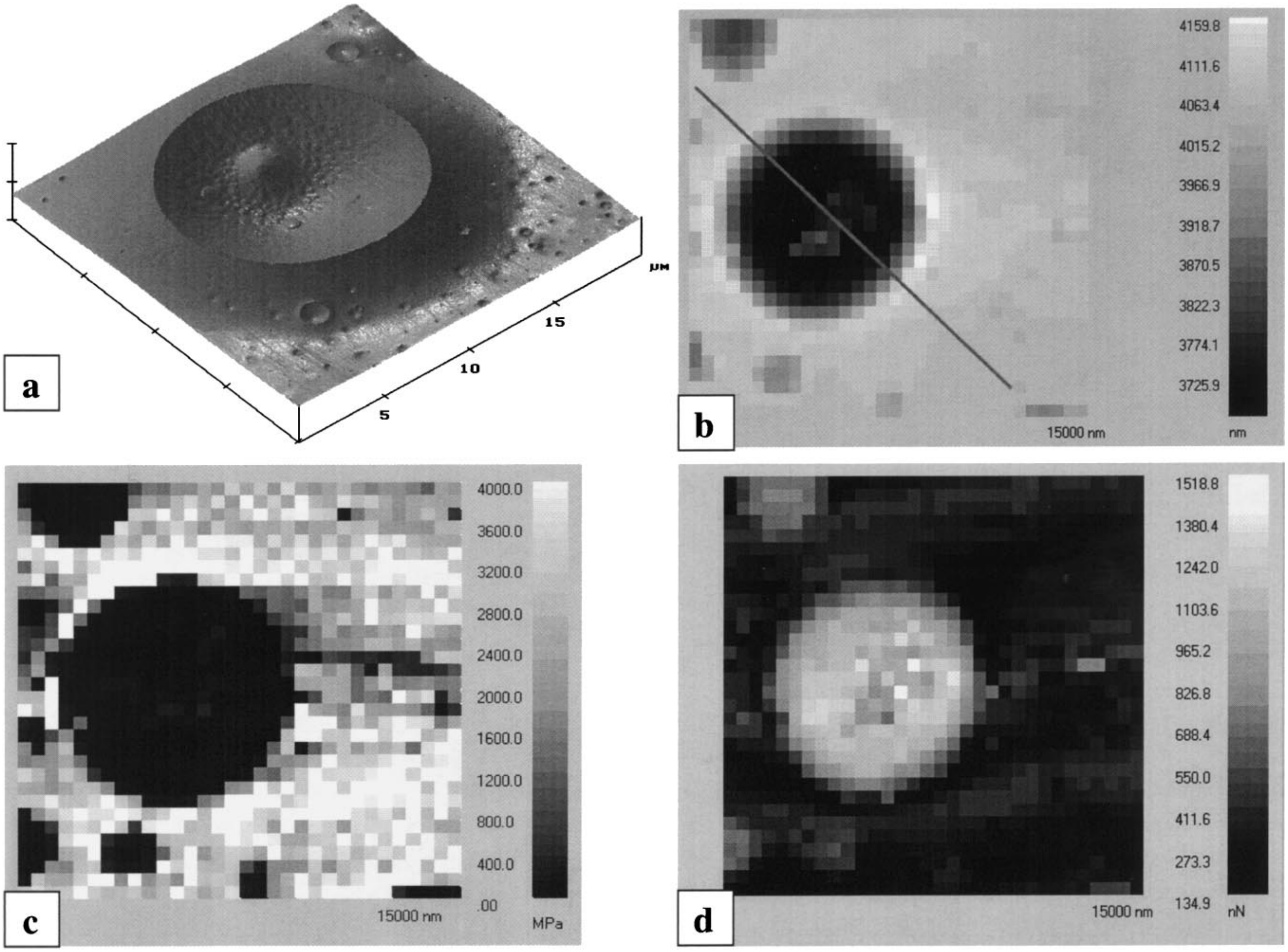

Fig. 1. (a) Topography of the PS/PB film with PB as the dispersed phase (20 μm × 20 μm, *z* scale is 1.5 μm). Pay attention to the dimension variation of the PB phase and the presence of the PS microphase inclusions inside of the larger PB droplet. Topography (b), elastic modulus (c), and adhesion (d) images of the same surface area of the PS/PB film (15 μm × 15 μm). Mappings are carried out with 32 × 32 pixels lateral resolution.

glassy matrix (Fig. 1a). The lateral size of the dispersed rubber phase varies from 20 μm to less than 1 μm and a different morphology (elevated or shallow droplets) is observed at various locations. Within the larger PB phase, submicron sized microinclusions of PS phase are frequently observed. Fig. 1b and c demonstrates the surface mapping (topography, elastic modulus, and adhesive forces) obtained concurrently for the same, 15 μm × 15 μm, surface area. It shows that for the rubber phase, the adhesive forces are much higher and the elastic modulus is much lower than for the PS matrix. Small rubber inclusions with lateral sizes less than 1 μm and microcracks propagating from rubber phase (right-hand side in Fig. 1b) can be also recognized in the elastic modulus and adhesive force micromappings.

A cross-section of the PB phase allows the direct observation of close correlations among surface properties as shown in Fig. 2. A topographical cross-section shows that the rubber phase is located within the 7-μm wide shallow region at 400 nm below the PS matrix surface. Young's modulus is around 2 GPa for the PS surface and drops sharply to below 10 MPa for the rubber phase (Fig. 2b). Finally, the adhesive forces, which are relatively small at the PS surface, increase three-fold for the rubber phase (Fig. 2c). Minor property variations follow the topography closely as can be seen from their singularities caused by a local elevation within the rubber phase (Fig. 2).

The histograms of the surface distribution of surface micromechanical properties display two very distinctive peaks (Fig. 3). For the surface distribution of elastic modulus, the first, very sharp peak is located in the range of 3–10 MPa and corresponds to the rubber phase (Fig. 3a). The broad distribution with a maximum around 2.5 GPa corresponds to the PS matrix. Absolute values obtained by the SPM probing are very close to those expected for the bulk material (about 3 MPa for PB and about 3 GPa for PS, both for 10 s tensile stress time [8]). Higher average value of elastic modulus observed for the rubber phase can be related to its confined state within thin films in the form of thin layers and droplets, a relatively short probing time, as well as the presence of some PS microinclusions inside larger PB droplets. On the contrary, a broad distribution and a lower average value of the elastic modulus for the

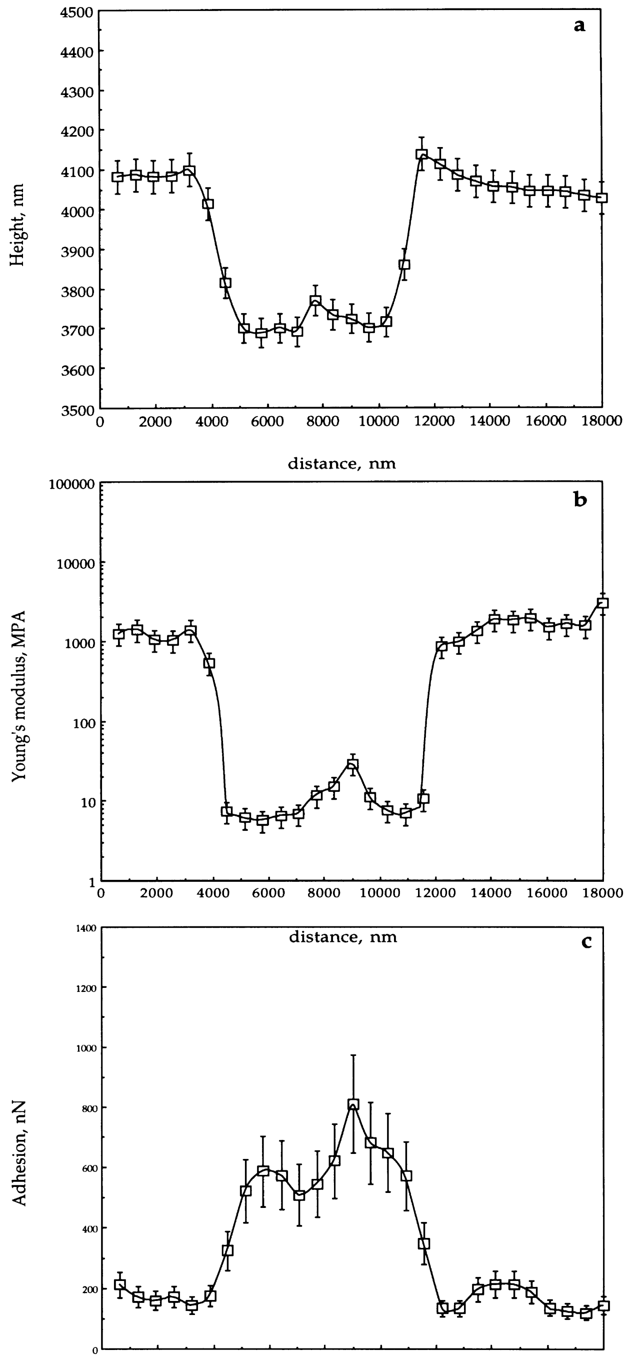

Fig. 2. Cross-sections of the rubber phase within the glassy matrix: (a) topography; (b) elastic modulus, pay attention to log-scale; and (c) adhesive force cross-sections (a section line is shown in Fig. 1b).

PS matrix is caused by the presence of multiple locations with lower modulus (very small and thin inclusions of the PB phase and microcracks with accumulated rubber material) and the PS/PB interface. The histogram of the distribution of adhesive forces (Fig. 3b) also shows very distinctive contributions of glassy and rubber phases with the PS matrix possessing much lower adhesion.

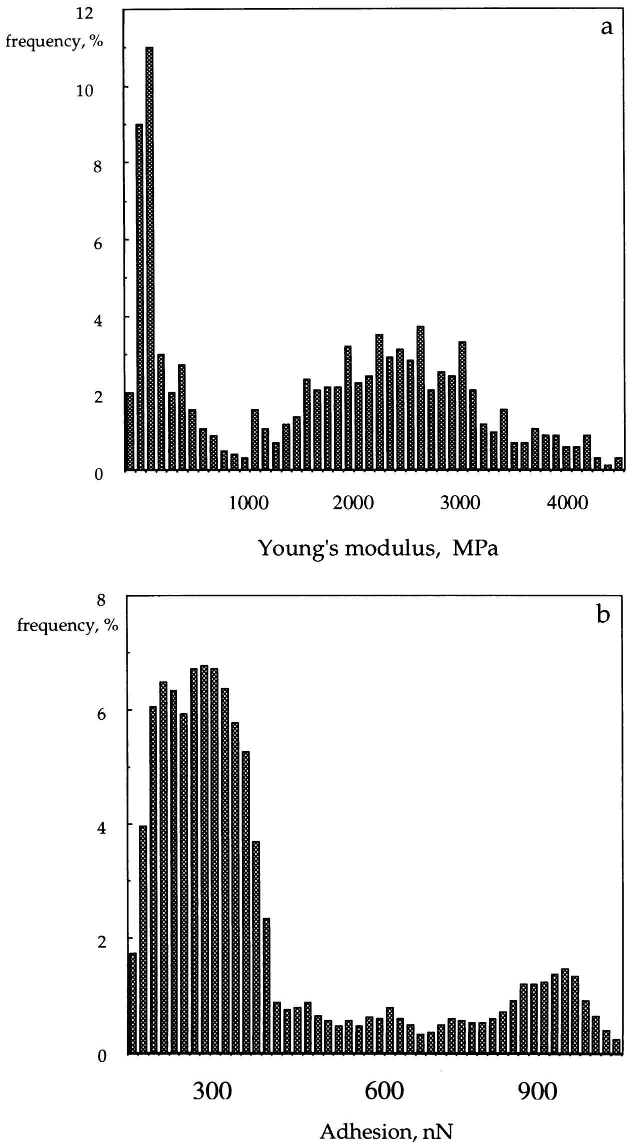

Fig. 3. Histograms of the surface distribution of: (a) elastic modulus; and (b) adhesive forces for the surface area in Fig. 1.

As we observed, this probing technique is also sensitive to the depth distribution of the elastic properties and can provide insight on the buried details of the surface distribution of different phases. As demonstrated in Fig. 4a, elastic modulus of the rubber phase shows the presence of the hard PS surface underneath the compliant material. The elastic modulus depth profile shows large variations at very low indentation depths (below 50 nm) caused, mainly, by the instability of the first contact as discussed in previous papers (see Refs. [12,13]). At larger indentation depths, a stable value of the elastic modulus is observed. However, at some indentation depth for the rubber phase, a sharp increase of the elastic modulus takes place (Fig. 4a). This is caused by the tip approaching the PS surface below the thin rubber layer. Therefore, this indentation depth indicates the thickness of a rubber phase at a particular location.

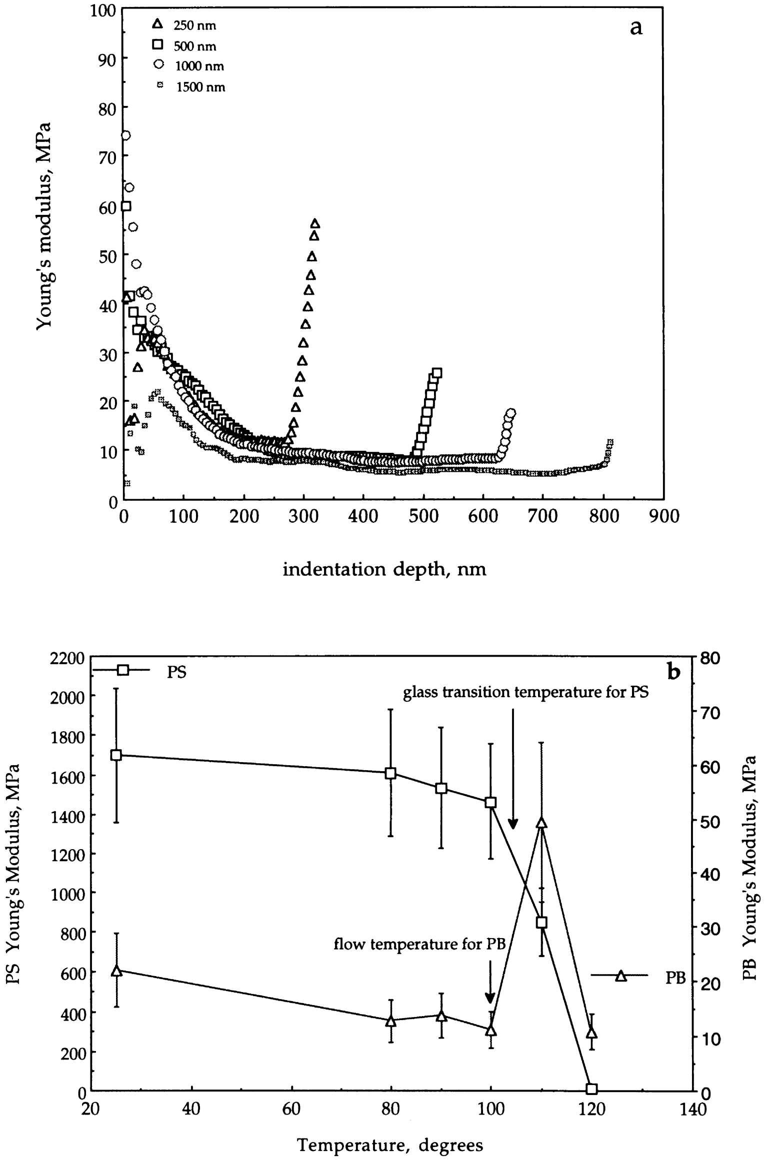

Fig. 4. (a) The depth profile of elastic moduli for the rubber phase at different distances from the glassy-rubber interface (shown in left top corner). (b) Temperature variations of elastic modulus for the PS matrix (left axis) and the PB phase (right axis).

Indeed, we observed a significant change in the rubber phase thickness from 250 nm for areas very close to the rubber–matrix interface to 800 nm in the central part of the rubber phase (see Fig. 4a for depth profiles at different distances from the PS/PB interface).

We measured the temperature dependence of elastic modulus separately for glassy and rubber phases (Fig. 4b). The absolute value of the elastic modulus for the PS phase decreases slightly (about 10%) from room temperature to about 100°C. A sharp drop in the elastic modulus to 11 MPa is observed within a narrow temperature interval of 100–120°C. This indicates that the glass transformation within a surface layer (probed to about 5 nm depth) occurs. The detected glass transition range correlates with the range determined for the bulk PS material ($T_g = 103$°C as measured for this sample by DSC).

On the contrary, the average elastic modulus of the rubber phase decreases steadily for temperatures up to 100°C (Fig. 4b). Its value increases sharply and unexpectedly around 110°C and then decreases again. This behavior can be understood after a careful analysis of the elastic modulus depth profiles. We estimated the elastic modulus by averaging over all indentation depths. At an elevated temperature, close to the flow temperature of the PB phase (100°C for PB with a given molecular mass [21]), the rubber phase losses its ability to elastic resistance. Thus, the SPM tip penetrates through the viscous phase and detects *only the PS surface*, which is still on the verge of transformation to the elastic state. This results in a sharp increase in the “integrated” elastic modulus value. Finally, at even higher temperatures, the PS matrix itself is transformed to the elastic state that causes a following drop in Young’s modulus. Young’s modulus underneath the PB phase at 120°C is 11 MPa, which equals the elastic modulus measured for the PS matrix at the same temperature.

In conclusion, we demonstrate that for the heterogeneous composite thin films fabricated from polymer blends, the micromapping of elastic properties can be obtained concurrently for glassy and rubber phases as well as across the interface with a lateral resolution better than 100 nm. Histograms of the surface distribution of elastic and adhesive properties display two very distinctive maxima, which allows *separate but concurrent measurements* of micromechanical properties of glassy and rubber phases in composite films. Depth profile measurements demonstrate a gradual increase of the rubber phase thickness with the increasing distance from the PS/PB interface. Both the glass transition temperature of the glassy matrix and the flow temperature of the rubber phase is determined to be close to bulk values.

Acknowledgements

This work is supported by The National Science Foundation, CMS-9610408 Grant and AFOSR F49620-93-C-0063 Contract. We appreciate technical support and discussions with S. Chizhik, V. Gorbunov, I. Luzinov, and J. Hazel.

References

[1] Binnig G, Quate CF, Gerber Ch. Phys Rev Lett 1986;12:930.
[2] Landman U, Luedtke WD, Burnham NA, Colton RJ. Science 1990;248:454.
[3] Burnham NA, Colton RJ. J Vac Sci Technol A 1989;7:2906.
[4] Oulevey F, Gremaud G, Semoroz A, Kulik AJ, Burnham NA, Dupas E, Gourdon D. Rev Sci Instrum 1998;69:2085.
[5] Marti O, Hild S. In: Tsukruk VV, Wahl K, editors. Microstructure and microtribology of polymer surfaces, ACS Symposium Series 1999;741:212.
[6] Radmacher M, Tillmann RW, Gaub HE. Biophys J 1993;64:735.
[7] Kajiyama T, Tanaka K, Takahara A. Macromolecules 1997;30:280.
[8] Aklonis JJ, MacKnight WJ. Introduction to polymer viscoelasticity. New York: Wiley, 1983.
[9] Vanlandingham MR, McKnight SH, Palmese GR, Ellings JR, Huang X, Bogetti TA, Eduljee RF, Gillespie JW. J Adhesion 1997;64:31.
[10] Overney R, Tsukruk VV. In: Ratner B, Tsukruk VV, editors. Scanning probe microscopy of polymers, ACS Symposium Series, vol. 694. 1998. p. 2.
[11] Domke J, Radmacher M. Langmuir 1998;14:3320.
[12] Chizhik SA, Huang Z, Gorbunov VV, Myshkin NK, Tsukruk VV. Langmuir 1998;14:2606.
[13] Tsukruk VV, Huang Z, Chizhik SA, Gorbunov VV. J Mater Sci 1998;33:4905.
[14] Huang Z, Chizhik SA, Gorbunov VV, Myshkin NK, Tsukruk VV. In: Tsukruk VV, Wahl K, editors. Microstructure and microtribology of polymer surfaces, ACS Symposium Series 1999;741:177.
[15] Tsukruk VV, Gorbunov VV, Huang Z, Chizhik SA. Polym Inte 2000 (accepted).
[16] Hazel JL, Tsukruk VV. J Tribol 1998;120:814.
[17] Hazel JL, Tsukruk VV. Thin Solid Films 1999;339:249.
[18] Huang Z. MS Thesis, Western Michigan University, 1999.
[19] Bliznyuk VN, Hazel JH, Wu J, Tsukruk VV. In: Ratner B, Tsukruk VV, editors. Scanning probe microscopy of polymers, vol. 694. 1998. p. 252.
[20] Huang Z, Tsukruk VV. In preparation.
[21] Vinogradov GV, Ozyara EA, Malkin AY, Grechanovskii VA. J Polym Sci A 1971;2(9):1153.